The global population of large craters on Mercury and comparison with the Moon

Caleb I. Fassett,[1] Seth J. Kadish,[1] James W. Head,[1] Sean C. Solomon,[2] and Robert G. Strom[3]

Received 28 February 2011; revised 4 April 2011; accepted 6 April 2011; published 17 May 2011.

[1] We have compiled a near-global catalog of impact craters on Mercury for diameters ≥20 km from images obtained during the flybys of the Mariner 10 and MESSENGER spacecraft. The observed variations in crater density suggest that the smooth plains within and around the Caloris basin are the most prominent contiguous, comparatively young regions on Mercury; no other comparably large area appears as young. In more heavily cratered terrain, even the most densely cratered regions on Mercury are deficient in craters between 20 km and ~100 km in diameter compared with the Moon, a result that extends an observation made from Mariner 10 images of a smaller fraction of Mercury's surface. This deficit is interpreted to reflect crustal resurfacing of Mercury early in its history, most likely by volcanic processes. For craters larger than ~100 km in diameter, the density of craters on Mercury in a given size range is similar to that of the Moon. Because such larger craters are less easily removed by volcanic resurfacing, we interpret this similarity to be the result of impact saturation effects on both bodies.
Citation: Fassett, C. I., S. J. Kadish, J. W. Head, S. C. Solomon, and R. G. Strom (2011), The global population of large craters on Mercury and comparison with the Moon, *Geophys. Res. Lett.*, *38*, L10202, doi:10.1029/2011GL047294.

1. Introduction

[2] The flybys of Mercury by the Mariner 10 and MErcury Surface, Space ENvironment, GEochemistry, and Ranging (MESSENGER) spacecraft have provided image coverage of >95% of the surface area of Mercury [*Becker et al.*, 2009]. The data returned to date are sufficient for an assessment of the cratering record over much of the surface of Mercury. We have constructed a near-global catalog of impact craters having diameters 20 km and larger. This catalog permits an assessment of first-order variations in crater density across nearly the entire surface of Mercury and a comparison with the global distribution of crater density on the Moon. This approach is complementary to detailed crater counting of specific regions [e.g., *Strom et al.*, 2008, 2011].

[1]Department of Geological Sciences, Brown University, Providence, Rhode Island, USA.
[2]Department of Terrestrial Magnetism, Carnegie Institution of Washington, Washington, D. C., USA.
[3]Lunar and Planetary Laboratory, University of Arizona, Tucson, Arizona, USA.

0094-8276/11/2011GL047294

2. Methods for Creating the Crater Catalog

[3] We began with the global image mosaic (~500-m/pixel) constructed by *Becker et al.* [2009] from a combination of images obtained with MESSENGER's Mercury Dual Imaging System (MDIS) [*Hawkins et al.*, 2007] and the Mariner 10 camera [*Murray*, 1975]. This mosaic was supplemented with additional data from Mariner 10 where its illumination geometry was preferable for crater identification. All data were imported into the ESRI ArcMap GIS environment with a Mercury datum of 2440 km radius. The *CraterTools* extension to ArcMap [*Kneissl et al.*, 2011] was used to mark craters and measure diameters. This program defines a best-fit circle to the crater rim from three points selected along the rim, or, alternatively, from drawing a rim-to-rim diameter. To assure accuracy, the diameter of each crater is computed in a sinusoidal projection with central meridian at the center of the crater.

[4] Craters on Mercury were mapped by overlaying a 20-km reference grid on the global mosaic and scanning systematically across the planet. Regions poleward of 70° latitude were examined separately in polar stereographic projections, and these data were then merged with the mid- and low-latitude data to produce the global dataset. This survey method was repeated at multiple scales to ensure that we detected all craters, from basins many hundreds of kilometers in diameter down to 20-km-diameter craters. The minimum diameter of 20 km was chosen to assure that the observed population consists principally of primary impact craters; earlier work suggests that secondary craters may be globally important up to ~10 km diameter on Mercury and that secondaries from large basins may locally be important even at diameters as large as ~20 km [*Strom et al.*, 2008, 2011]. This minimum size is also well above the resolution limits for the data that make up the global mosaic. All visible craters were counted, regardless of their degradation states or whether they were partially buried by surface units. In all, 6040 craters with diameter ≥20 km were mapped across the total imaged area of 7.31×10^7 km^2 (Figure 1a), representing more than 95% of the surface area of Mercury.

[5] Analysis of the observed crater population requires an understanding of the influence of variations in observation and illumination conditions on the ability to recognize craters and basins in images. Solar incidence angle plays a particularly important role in crater recognition [e.g., *Soderblom*, 1972; *Wilcox et al.*, 2005]. Overhead or direct solar illumination severely reduces the ability to discern subtle topography and often makes it impossible to recognize degraded craters; indeed, some craters may become apparent only with detailed topography [e.g., *Frey et al.*, 1999]. For this reason,

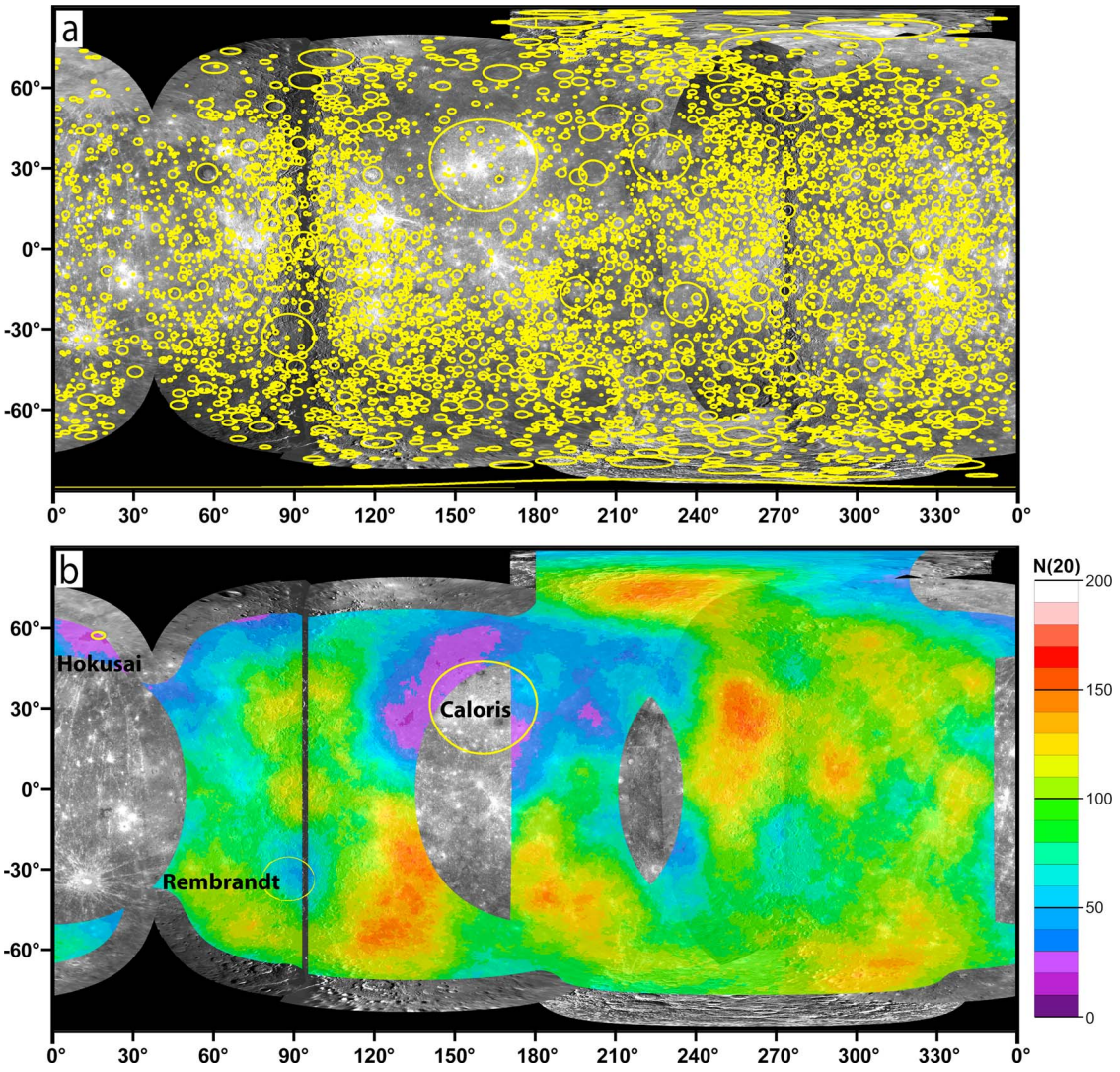

Figure 1. (a) Outlines of craters mapped on the surface of Mercury overlain on the global mosaic of Mercury from MESSENGER and Mariner 10 images [*Becker et al.*, 2009]. (b) Crater density $N(20)$ on Mercury calculated for neighborhoods of radius 500 km. Regions without colors were eliminated on the basis of low solar incidence angle or high emission angle. Note the lower crater density in the region around the Caloris basin (~0° to 60°N, 120° to 210°E). Maps are in equidistant cylindrical projection with a Mercury datum of 2440 km radius.

we limited our quantitative analysis to regions where images were taken at solar incidence angle $i > 50°$ (measured from nadir). We also masked out observations taken near the limb of the planet by excluding areas imaged with emission angle $e > 75°$ (measured from nadir). These parameters were chosen by examining how crater size-frequency distribution varies as a function of incidence and emission angle and setting the masking threshold to eliminate areas most affected by observational biases (see additional discussion in Text S1 of the auxiliary material).[1] A more stringent observational mask ($i > 60°$, $e < 65°$) did not substantially alter the qualitative or quantitative conclusions of this paper. Given our observational criteria, the total area on Mercury available is 5.22×10^7 km^2 (~70% of the surface area), for which 4924 craters of diameter ≥20 km appear in the catalog.

3. Geographic Distribution of Craters on Mercury

[6] With the new crater catalog (Figure 1a), we determined the areal density of craters on Mercury by calculating the number of craters in a moving neighborhood 500 km in radius centered on each pixel (at 2 pixels per degree) (Figure 1b). The resulting crater densities are interpreted to reflect variations in the large-scale crater retention age (for 20-km-diameter craters and larger) across the surface. We report densities here as $N(D)$, where N is the number of craters of diameter D or greater per 10^6 km^2 area. The neighborhood size was chosen to be sufficiently large to assure that observed variations are a result of geological differences rather than counting statistics (see auxiliary material). No

[1] Auxiliary materials are available in the HTML. doi:10.1029/2011GL047294.

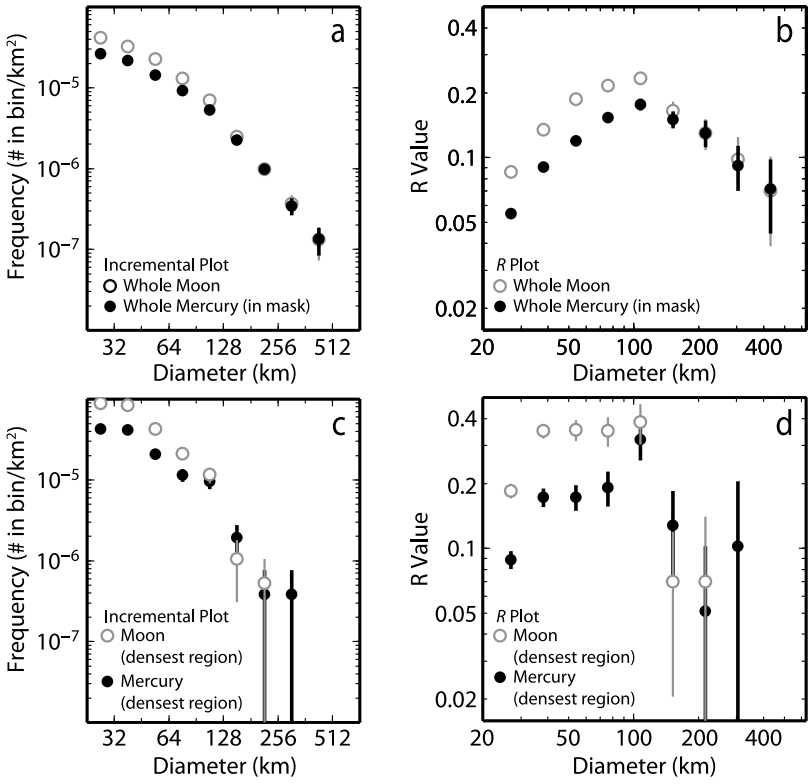

Figure 2. (a) Incremental plot and (b) *R* plot [see *Crater Analysis Techniques Working Group*, 1978] of the spatial density of craters on Mercury for regions meeting our observational requirements and for the entire Moon [*Head et al.*, 2010]. At large diameters, the crater densities on both surfaces are similar, but they differ substantially for craters having diameters smaller than ~128 km. (c, d) Crater size-frequency distributions on the most densely cratered portions of Mercury and the Moon, i.e., areas for which $N(20)$ fell within the upper 5% of values on each body. Because Mercury has fewer craters of D ~20 km than the Moon, the most densely cratered 5% of the measured area has $N(20) > 132$, whereas on the Moon, this most densely cratered 5% has $N(20) > 237$. Errors shown are from $(n \pm \sqrt{n})$/area, where n is the number of craters in the size bin.

correction of neighborhood density was made at the edges of our excluded region; for this reason, regions closest to those edges have greater uncertainties. This effect falls off rapidly with distance from the edges of the mask.

[7] The most prominent feature in Figure 1b is the obvious contrast in crater density between the immediate surroundings of the Caloris basin and most other regions on Mercury. The fact that the smooth plains east of Caloris, as well as on its eastern interior third, have fewer craters than other regions and are therefore younger has been known since Mariner 10 [*Murray et al.*, 1975]. This observation has been re-examined with MESSENGER data and expanded to previously unimaged areas [*Murchie et al.*, 2008; *Strom et al.*, 2008; *Fassett et al.*, 2009]. The Caloris plains have a characteristic $N(20)$ of ~25, although some variation about this density exists. Local crater counts that include smaller craters imply that the heterogeneity in crater density seen around the basin primarily reflects differences in the thickness of plains and thus the degree to which pre-existing craters on the plains were obliterated, rather than differences in the timing of plains emplacement [e.g., *Fassett et al.*, 2009, Figures 8E and 8F].

[8] The comparative youthfulness and large expanse of the Caloris smooth plains appear to be unusual on Mercury. No other plains units of similar size (>10^6 km^2 in extent) and similar low crater density [$N(20)$ <30] are observed. Other regions of note in the $N(20)$ crater statistics map (Figure 1b) include the area in and around the Rembrandt basin, which is similar in age to the Caloris basin [*Watters et al.*, 2009]. The apparent resurfacing within and around the Rembrandt basin provides further evidence for emplacement of volcanic plains in its interior and surroundings, although those plains appear to be somewhat older than the plains associated with Caloris [*Watters et al.*, 2009]. The region around the 95-km-diameter rayed crater Hokusai (58°N, 17°E), also known as radar feature B [e.g., *Harmon et al.*, 2007], and nearby plains in the north polar region also appear to have fewer craters per area than average (Figure 1b). Current data imply that this expanse may be the second largest area of comparatively young smooth plains on Mercury.

4. Comparison Between Mercury and the Moon

[9] The average density of craters on Mercury can be assessed independent of specific geological units by plotting the crater size-frequency distribution for the entire planet (taking into account the observational mask described above). A similar assessment of global crater densities has been made for the Moon [*Head et al.*, 2010] from a catalog derived from topography measurements by the Lunar Orbiter Laser Altimeter (LOLA) [*Smith et al.*, 2010]. Although the catalogs derived from images and altimetry have some differences in observational characteristics and completeness, comparisons of past catalog data have found generally good agreement between density measurements at the ~20% level (e.g., the

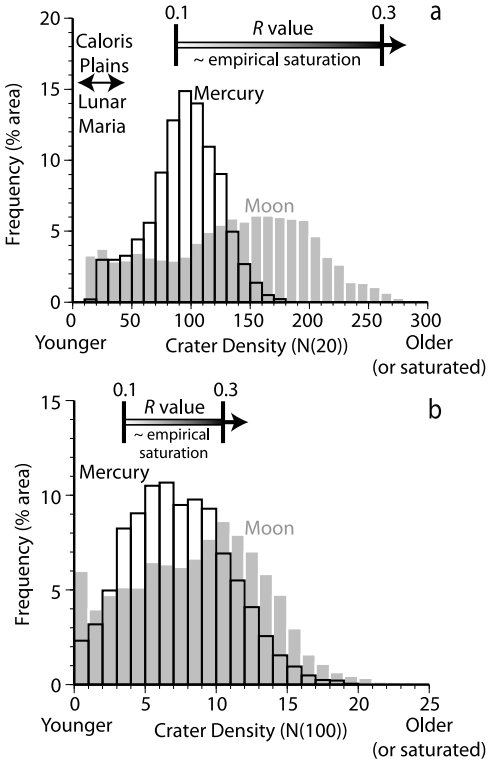

Figure 3. Frequency distributions of areas of a given crater density, for craters of diameter (a) $D \geq 20$ km and (b) $D \geq 100$ km (over measurement areas ~10^6 km^2 in moving neighborhoods of 500 km radius on both bodies). R values (0.1–0.3) that reflect saturation densities are from the models of *Richardson* [2009]. The areas with $N(20)$ values marked by the arrow in Figure 3a occur only in the lunar maria or the vicinity of Caloris on Mercury. At $D \geq 100$ km, both surfaces may have generally reached saturation early in their history; the area with $R > 0.1$ on both bodies is substantial, 82% of the surface area on the Moon and 85% for Mercury.

comparison of data from *Strom et al.* [2005] with those from *Head et al.* [2010]). For the crater size range described here, the primary difference is that altimetry leads to a systematic improvement in crater recognition of ~10–30%, with the largest differences in densely cratered regions.

[10] "Whole planet" crater size-frequency distributions for the Moon and Mercury are plotted in Figure 2. These data are shown in two formats: as an incremental frequency plot, which is a histogram of crater density within a given size range, and as an R plot, which normalizes differential crater frequency relative to a D^{-3} power law, an operation that helps discriminate clearly between crater populations of different size distributions [see *Crater Analysis Techniques Working Group*, 1978]. For both plots, we follow the common convention that boundaries of individual crater-diameter bins are multiples of $\sqrt{2}$.

[11] Two main observations come from comparison of these two catalogs (Figure 2). First, in the diameter range 128 km to 512 km, Mercury has virtually the same density of craters as the Moon (Figures 2a and 2b). Second, at smaller diameters, the shape of the crater size-frequency distribution on Mercury is similar to that of the Moon, but the density of craters on Mercury between $D = 20$ km and $D = 128$ km is lower than on the Moon by approximately one-third [see also *Strom*, 1977; *Strom et al.*, 2011]. This difference is substantial and beyond what might be traced to the different sources of the base maps used to create each catalog. The global $N(20)$ values for the two planetary bodies are 94 on Mercury (4924 craters in 5.217×10^7 km^2) and 137 on the Moon (5185 craters in 3.793×10^7 km^2).

[12] To assess further the difference between the Moon and Mercury, we examined the regions with the highest crater density on each planet. We selected the most densely cratered 5% of each surface as specified from $N(20)$ values. The crater size-frequency distributions for these densest regions (Figures 2c and 2d) are broadly consistent with the global distributions: at diameters larger than ~128 km, the surfaces are indistinguishable within error, but for smaller-diameter craters ($D = 20$ to 100 km), in the most densely cratered regions of each planet, Mercury has a crater density 50% that of the Moon. This difference is also manifested in the frequency distribution of terrain at various levels of cratering (Figure 3). More than 30% of the lunar surface has $N(20) > 170$, but essentially no terrain on Mercury has $N(20)$ values this high (in measurement neighborhoods of ~10^6 km^2 area). This contrast in densities at these crater sizes is also consistent with Mariner 10 observations over ~40% of Mercury's surface [*Strom*, 1977; *Spudis and Guest*, 1988; *Strom and Neukum*, 1988].

5. Discussion

5.1. Young Terrains on the Moon and Mercury

[13] To understand the crater size-frequency distributions in Figures 2a and 2b that describe the global cratering of the Moon and Mercury, we first ask the question: How important has late-stage volcanic resurfacing been on each planet? One way to examine this question is to determine the fraction of surface area with $N(100) > 3.5$ ($R > 0.1$ on an R plot [see *Crater Analysis Techniques Working Group*, 1978]), which is similar on both bodies (82% on the Moon and 85% within the count area on Mercury) (Figure 3b). The only large, contiguous regions with $N(100)$ below this value in our data are the nearside lunar maria and the plains surrounding Caloris. This result suggests that the resurfacing histories of the Moon and Mercury subsequent to the period of heavy bombardment were similar, with ~15–20% of the area resurfaced by younger volcanism.

5.2. Density of Large Craters on Mercury and the Moon

[14] Our data show that the density of craters with diameters in the range ~128–512 km is similar on Mercury and the Moon. This conclusion differs somewhat from that reported from Mariner 10 observations by *Strom and Neukum* [1988] (*Strom and Neukum* [1988, Figure 9] show fewer craters in the heavily cratered terrain on Mercury than the lunar highlands, although their statistics for diameters > 100 km on Mercury were poor). Two possible explanations for the similarity between the Moon and Mercury at large sizes are: (1) cratering of both surfaces reached saturation equilibrium at these crater sizes, or (2) neither body was saturated and both surfaces have the same time-integrated cratering flux (to within error).

[15] Saturation equilibrium is reached when accumulating craters (and their ejecta) are effectively obliterating as many pre-existing craters as are formed [*Gault*, 1970; *Marcus*,

1970]. However, whether saturation is actually observed on solar system surfaces is a subject of sustained debate [*Marcus*, 1970; *Woronow*, 1977; *Hartmann*, 1984; *Chapman and McKinnon*, 1986; *Strom and Neukum*, 1988; *Hartmann*, 1995; *Hartmann and Gaskell*, 1997].

[16] Recent modeling of how crater populations accumulate has added new evidence that craters are at saturation levels in the lunar highlands, with densities occurring at R values of ~0.1 to 0.3 [*Richardson*, 2009]. Because our data suggest that (1) Mercury has the same density of large craters as the Moon, and (2) both the Moon and Mercury have R values > 1 for ~100-km-diameter craters over more than 80% of their surfaces, we suggest that saturation was reached on Mercury as well as the Moon. As we discuss in the following section, however, craters at small diameters are more readily removed, and they appear to have experienced a different history.

[17] A further implication of *Richardson*'s [2009] modeling study is that the shape of the crater size-frequency distribution can continue to reflect the accumulating population even in saturation, as originally suggested by *Chapman and McKinnon* [1986]. This result implies that it may be impossible to rely on the shape of the size-frequency distribution alone to decide whether saturation has been reached. Thus, the Moon and Mercury may both have been saturated at large crater diameters (Figure 2), although models suggest that preservation of a saturated population may be inconsistent with the steepness of the production function in this size-range [*Chapman and McKinnon*, 1986; *Richardson*, 2009].

[18] Alternatively, the similar crater size-frequency distributions for the Moon and Mercury at large crater diameters may simply be a result of both planetary bodies having had the same time-integrated flux at these crater sizes. This explanation is plausible because the shape of the production function on ancient terrains of the Moon and Mercury was similar [*Strom et al.*, 2005, 2008]. However, for this explanation to be correct in the absence of saturation, the product of the period of surface exposure and rate of large crater formation must be the same for both surfaces, which would constitute a remarkable coincidence, especially given that models for the rate of crater formation on Mercury imply faster crater accumulation than on the Moon [*Marchi et al.*, 2009; *Massironi et al.*, 2009].

[19] An additional factor that may have been important in reaching similar crater densities on the Moon and Mercury is crater removal by processes other than later cratering. It is possible that both planetary bodies reached saturation by large craters, but the crater size-frequency distribution on both bodies subsequently was modified by volcanism or other geological processes to approximately the same degree. This explanation is consistent with the similar fractional areas of young terrain on both bodies ($R < 0.1$) (Figure 3b).

[20] In sum, our observations are consistent with the hypothesis that crater saturation was reached for craters of diameter $D > 128$ km on both Mercury and the Moon. Deciding whether this or another explanation is correct will require new observations of crater density and improvements in modeling of how crater populations accumulate.

5.3. Deficit of Craters on Mercury and the Moon at Diameters 20 to 128 km

[21] The deficit in crater density at diameters 20 to 128 km on Mercury compared with the Moon was recognized from Mariner 10 data [*Strom*, 1977; *Spudis and Guest*, 1988; *Strom and Neukum*, 1988]. Hypotheses that might explain this deficit on Mercury include: (1) differences in the population of impactors on the two bodies; (2) differences in scaling related to differences in surface gravitational acceleration, strength of the target, or impact velocity; (3) differences in how secondary versus primary craters contributed to the surface population, particularly secondary craters from basin formation; and (4) differences in resurfacing that affected how crater populations accumulated and were preserved on the two surfaces. However, because models suggest Mercury has the same impactor population and a similar cratering efficiency to the Moon [*Strom et al.*, 2005; *Marchi et al.*, 2009], the first two explanations are unlikely. Variations in the secondary cratering process are also unlikely to explain this difference, because secondary craters are more common on Mercury than the Moon [*Strom et al.*, 2008, 2011], not less, and most secondaries are smaller than the size range of craters considered here.

[22] The hypothesis that the deficit of small craters on Mercury is a result of resurfacing is thus preferred. Such a difference is plausibly the result of widespread emplacement of intercrater plains on Mercury early in its history [e.g., *Trask and Guest*, 1975; *Murray et al.*, 1975; *Malin*, 1976; *Strom*, 1977; *Leake*, 1982]. Superposition relationships and crater statistics both provide evidence that such emplacement was not a short-lived episode but rather a complex sequence of resurfacing events during the period when rates of impact cratering were high [*Malin*, 1976; *Woronow and Love*, 1987].

[23] From images of terrains with the highest $N(20)$ values on both the Moon and Mercury (Figure S1), it is clear that the most densely cratered regions on Mercury have smoother inter-crater surfaces than the most densely cratered regions of the Moon. Heavily cratered areas on Mercury tend to be intimately interspersed with intercrater plains that are not readily separable stratigraphically [*Trask and Guest*, 1975]. Thus, we favor the hypothesis that the difference in crater densities between the Moon and Mercury at these crater sizes is due to plains formation concomitant with early cratering [e.g., *Strom*, 1977], and that even the most densely cratered terrains on Mercury have experienced significant erasure of craters. This hypothesis implies that Mercury experienced crustal resurfacing early in its history on essentially a global basis, in contrast with the Moon, which has crater-saturated highlands regions that were never resurfaced. If intercrater plains on Mercury are volcanic in origin, this interval of global resurfacing has important implications for the thermal evolution of Mercury. Such a view is consistent with the idea [e.g., *Denevi et al.*, 2009] that the upper crust of Mercury is dominated by volcanic sequences of various ages and that no "primary" crust [*Taylor*, 1989] is exposed at the surface today.

6. Conclusions

[24] Global analysis of the impact cratering record on Mercury from Mariner 10 and MESSENGER images suggests that the circum-Caloris smooth plains are the largest, contiguous region of comparatively young, smooth plains and that no other comparably young terrain is as widespread. Comparison of the crater populations of Mercury and the Moon supports inferences from Mariner 10 observations that Mercury is deficient in craters with diameters between 20 and

~100 km compared with the Moon, even in its most heavily cratered regions. The most plausible hypothesis for this deficit is intercrater plains emplacement. In contrast, at crater diameters larger than ~100 km, a similar density of craters is observed on Mercury and the Moon. This result is plausibly the consequence of saturation having been reached on both bodies. High-resolution observations to be obtained during the orbital phase of the MESSENGER mission will be invaluable for extending and further analyzing Mercury's cratering record and its interpretation.

[25] **Acknowledgments.** Reviews by Matteo Massironi and an anonymous reviewer helped improve this manuscript. We thank Thomas Kneissl for developing and sharing the extraordinarily useful CraterTools extension to ArcMap. Comments and assistance from Clark Chapman, David Blewett, Jay Dickson, and Debra Hurwitz are gratefully acknowledged. We also thank Kris Becker, Tammy Becker, Lynn Weller, Scott Turner, Lillian Nguyen, Christina Selby, Mark Robinson, and Brett Denevi for creating the mosaic of Mercury after the third MESSENGER flyby. The MESSENGER project is supported by the NASA Discovery Program under contracts NAS5-97271 to the Johns Hopkins University Applied Physics Laboratory and NASW-00002 to the Carnegie Institution of Washington.

[26] The Editor thanks Matteo Massironi and an anonymous reviewer for their assistance in evaluating this paper.

References

Becker, K. J., M. S. Robinson, T. L. Becker, L. A. Weller, S. Turner, L. Nguyen, C. Selby, B. W. Denevi, S. L. Murchie, R. L. McNutt, and S. C. Solomon (2009), Near global mosaic of Mercury, *Eos. Trans. AGU*, *90*(52), Fall Meet. Suppl., Abstract P21A-1189.

Chapman, C. R., and W. B. McKinnon (1986), Cratering of planetary satellites, in *Satellites*, edited by J. A. Burns and M. S. Matthews, pp. 492–580, Univ. of Ariz. Press, Tucson.

Crater Analysis Techniques Working Group (1978), Standard techniques for presentation and analysis of crater size-frequency data, *Tech. Memo. 79730*, 24 pp., NASA, Washington, D. C.

Denevi, B. W., et al. (2009), The evolution of Mercury's crust: A global perspective from MESSENGER, *Science*, *324*, 613–618.

Fassett, C. I., J. W. Head, D. T. Blewett, C. R. Chapman, J. L. Dickson, S. L. Murchie, S. C. Solomon, and T. R. Watters (2009), Caloris impact basin: Exterior geomorphology, stratigraphy, morphometry, radial sculpture, and smooth plains deposits, *Earth Planet. Sci. Lett.*, *285*, 297–308, doi:10.1016/j.epsl.2009.05.022.

Frey, H. V., S. E. H. Sakimoto, and J. H. Roark (1999), Discovery of a 450 km diameter, multi-ring basin on Mars through analysis of MOLA data, *Geophys. Res. Lett.*, *26*, 1657–1660, doi:10.1029/1999GL900357.

Gault, D. E. (1970), Saturation and equilibrium conditions for impact cratering on the lunar surface: Criteria and implications, *Radio Sci.*, *5*, 273–291, doi:10.1029/RS005i002p00273.

Harmon, J. K., M. A. Slade, B. J. Butler, J. W. Head, M. S. Rice, and D. B. Campbell (2007), Mercury: Radar images of the equatorial and midlatitude zones, *Icarus*, *187*, 374–405, doi:10.1016/j.icarus.2006.09.026.

Hartmann, W. K. (1984), Does crater "saturation equilibrium" occur in the solar system?, *Icarus*, *60*, 56–74, doi:10.1016/0019-1035(84)90138-6.

Hartmann, W. K. (1995), Planetary cratering 1. The question of multiple impactor populations: Lunar evidence, *Meteoritics*, *30*, 451–467.

Hartmann, W. K., and R. W. Gaskell (1997), Planetary cratering 2: Studies of saturation equilibrium, *Meteorit. Planet. Sci.*, *32*, 109–121, doi:10.1111/j.1945-5100.1997.tb01246.x.

Hawkins, S. E., II, et al. (2007), The Mercury Dual Imaging System on the MESSENGER spacecraft, *Space Sci. Rev.*, *131*, 247–338, doi:10.1007/s11214-007-9266-3.

Head, J. W., C. I. Fassett, S. J. Kadish, D. E. Smith, M. T. Zuber, G. A. Neumann, and E. Mazarico (2010), The distribution of large lunar craters: Implications for resurfacing and impactor populations, *Science*, *329*, 1504–1507, doi:10.1126/science.1195050.

Kneissl, T., S. van Gasselt, and G. Neukum (2011), Map-projection-independent crater size-frequency determination in GIS environments—New software tool for ArcGIS, *Planet. Space Sci.*, doi:10.1016/j.pss.2010.03.015, in press.

Leake, M. A. (1982), The intercrater plains of Mercury and the Moon: Their nature, origin, and role in terrestrial planet evolution, *Tech. Memo. 84894*, pp. 3–535, NASA, Washington, D. C.

Malin, M. C. (1976), Observations of the intercrater plains of Mercury, *Geophys. Res. Lett.*, *3*, 581–584, doi:10.1029/GL003i010p00581.

Marchi, S., S. Mottola, G. Cremonese, M. Massironi, and E. Martellato (2009), A new chronology for the Moon and Mercury, *Astron. J.*, *137*, 4936–4948, doi:10.1088/0004-6256/137/6/4936.

Marcus, A. H. (1970), Comparison of equilibrium size distributions for lunar craters, *J. Geophys. Res.*, *75*, 4977–4984, doi:10.1029/JB075i026p04977.

Massironi, M., G. Cremonese, S. Marchi, E. Martellato, S. Mottola, and R. J. Wagner (2009), Mercury's geochronology revised by applying Model Production Function to Mariner 10 data: Geological implications, *Geophys. Res. Lett.*, *36*, L21204, doi:10.1029/2009GL040353.

Murchie, S. L., et al. (2008), Geology of the Caloris basin, Mercury: A view from MESSENGER, *Science*, *321*, 73–76, doi:10.1126/science.1159261.

Murray, B. C. (1975), The Mariner 10 pictures of Mercury: An overview, *J. Geophys. Res.*, *80*, 2342–2344, doi:10.1029/JB080i017p02342.

Murray, B. C., R. G. Strom, N. J. Trask, and D. E. Gault (1975), Surface history of Mercury: Implications for the terrestrial planets, *J. Geophys. Res.*, *80*, 2508–2514, doi:10.1029/JB080i017p02508.

Richardson, J. E. (2009), Cratering saturation and equilibrium: A new model looks at an old problem, *Icarus*, *204*, 697–715, doi:10.1016/j.icarus.2009.07.029.

Smith, D. E., et al. (2010), The Lunar Orbiter Laser Altimeter investigation on the Lunar Reconnaissance Orbiter mission, *Space Sci. Rev.*, *150*, 209–241, doi:10.1007/s11214-009-9512-y.

Soderblom, L. A. (1972), The process of crater removal in the lunar maria, in *Apollo 15 Preliminary Science Report*, *Spec. Publ. SP-289*, pp. 87–91, NASA, Washington, D. C.

Spudis, P. D., and J. E. Guest (1988), Stratigraphy and geologic history of Mercury, in *Mercury*, edited by F. Vilas, C. R. Chapman, and M. S. Matthews, pp. 118–164, Univ. of Ariz. Press, Tucson.

Strom, R. G. (1977), Origin and relative age of lunar and Mercurian intercrater plains, *Phys. Earth Planet. Inter.*, *15*, 156–172, doi:10.1016/0031-9201(77)90028-0.

Strom, R. G., and G. Neukum (1988), The cratering record on Mercury and the origin of impacting objects, in *Mercury*, edited by F. Vilas, C. R. Chapman, and M. S. Matthews, pp. 336–373, Univ. of Ariz. Press, Tucson.

Strom, R. G., R. Malhotra, T. Ito, F. Yoshida, and D. A. Kring (2005), The origin of planetary impactors in the inner solar system, *Science*, *309*, 1847–1850, doi:10.1126/science.1113544.

Strom, R. G., C. R. Chapman, W. J. Merline, S. C. Solomon, and J. W. Head (2008), Mercury cratering record viewed from MESSENGER's first flyby, *Science*, *321*, 79–81, doi:10.1126/science.1159317.

Strom, R. G., M. Banks, C. R. Chapman, C. I. Fassett, J. A. Forde, J. W. Head, W. J. Merline, L. M. Prockter, and S. C. Solomon (2011), Mercury crater statistics from MESSENGER flybys: Implications for stratigraphy and resurfacing history, *Planet. Space Sci.*, in press.

Taylor, S. R. (1989), Growth of planetary crust, *Tectonophysics*, *161*, 147–156, doi:10.1016/0040-1951(89)90151-0.

Trask, N. J., and J. E. Guest (1975), Preliminary geologic terrain map of Mercury, *J. Geophys. Res.*, *80*, 2461–2477, doi:10.1029/JB080i017p02461.

Watters, T. R., J. W. Head, S. C. Solomon, M. S. Robinson, C. R. Chapman, B. W. Denevi, C. I. Fassett, S. L. Murchie, and R. G. Strom (2009), Evolution of the Rembrandt impact basin on Mercury, *Science*, *324*, 618–621.

Wilcox, B. B., M. S. Robinson, P. C. Thomas, and B. R. Hawke (2005), Constraints on the depth and variability of the lunar regolith, *Meteorit. Planet. Sci.*, *40*, 695–710, doi:10.1111/j.1945-5100.2005.tb00974.x.

Woronow, A. (1977), Crater saturation and equilibrium: A Monte Carlo simulation, *J. Geophys. Res.*, *82*, 2447–2456, doi:10.1029/JB082i017p02447.

Woronow, A., and K. M. Love (1987), Mercurian crater-filling classes constrain the emplacement process of the intercrater plains material, *Icarus*, *71*, 376–385, doi:10.1016/0019-1035(87)90035-2.

C. I. Fassett, J. W. Head, and S. J. Kadish, Department of Geological Sciences, Brown University, Providence, RI 02912, USA. (caleb_fassett@brown.edu)

S. C. Solomon, Department of Terrestrial Magnetism, Carnegie Institution of Washington, Washington, DC 20015, USA.

R. G. Strom, Lunar and Planetary Laboratory, University of Arizona, Tucson, AZ 85721, USA.